Patterned Colloid Assembly by Grafted Photochromic Polymer Layers

Martin Piech,[†] Matthew C. George,[‡] Nelson S. Bell,*[,†] and Paul V. Braun*[,‡]

Sandia National Laboratories, Albuquerque, New Mexico 87185, and Department of Materials Science and Engineering, Frederick Seitz Materials Research Laboratory, and Beckman Institute for Advanced Science and Technology, University of Illinois at Urbana-Champaign, Urbana, Illinois 61801

Received June 17, 2005. In Final Form: November 8, 2005

Quartz surfaces and colloidal silica particles were derivatized with a poly(methyl methacrylate) copolymer containing spirobenzopyran (SP) photochromic molecules in the pendant groups at a concentration of 20 mol %. Two-photon near-IR excitation (∼780 nm) was then used to create chemically distinct patterns on the modified surfaces through a photochromic process of SP transformation to the zwitterionic merocyanine (MC) isomer. The derivatized colloids were approximately 10 times more likely to adsorb onto the photoswitched, MC regions. Surface coverage and adsorption kinetics have been compared to the mean-field model of irreversible monolayer adsorption.

"Bottom-up" or self-assembly strategies for the formation of colloidal heterostructures have great potential applications in photonic devices and microfluidics.[1] Directing colloidal deposition onto specific regions of a surface with high selectivity and ease remains an experimental challenge. Several approaches have been developed to this end, including lithographic fabrication of microwells and microtrenches,[2,3] photolithography of self-assembled monolayers,[4−6] microcontact printing,[7] dip-pen nanolithography,[8] utilization of copolymer phase separation,[9] and application of external optical,[10,11] electrical,[12] and magnetic[13] fields. However, in most of these approaches, processing times for surface preparation are lengthy, and deposition is not exclusive to the patterned regions. It should be mentioned that patterned substrates have also been utilized in the past for templated growth of colloidal crystals.[3,14−17]

In this work we present observations of colloidal patterning based on photoswitching of photosensitive polymer derivatized surfaces. These polymers impart capabilities for colloidal deposition using remote, light-actuated stimuli. This novel deposition method does not rely on traditional lithographic techniques or microcontact stamping to modify the chemical functionality of the substrate. Furthermore, the application of optical interferometry techniques should enable straightforward formation of highly ordered 2-D patterns over large surface areas.

The synthesis of polymerically derivatized photosensitive particles is detailed elsewhere.[18] In brief, silica colloids were first modified with a radical initiator monolayer[19] and then coated with a spirobenzopyran-*co*-methyl methacrylate (SP-*co*-MMA) copolymer brush containing 20 mol % of SP units in pendant groups (step 1 in Figure 1) using atom transfer radical polymerization (ATRP).[20−22] Quartz surfaces were modified by an identical procedure. Transmission electron microscopy (TEM) and atomic force microscopy studies revealed that both quartz substrates and particles were uniformly coated by the polymer layer with a typical root-mean-squared roughness of 2.2 nm over a 100 μm^2 area. The dry layer thicknesses of the polymer coating on the particles and substrates were determined to be 27 and 75 nm, respectively, using TEM measurements of particles with polymer layers grown under identical conditions.

Figure 1 presents a graphic outline of the ATRP growth procedure and the spirobenzopyran−merocyanine (SP−MC) photochemistry.[23] Exposure of the SP molecule to UV (366 nm) radiation induces ring-opening isomerization, giving the zwitterionic MC form (step 2 in Figure 1). The reverse isomerization reaction occurs slowly at room temperature, but can be accelerated by 585 nm light (step 2′ in Figure 1). Upon the SP-to-MC conversion, the SP-*co*-MMA-copolymer-modified colloids undergo a color transition from light yellow to purple/red in toluene. Simultaneously, rapid aggregation and sedimentation occur as reported elsewhere,[24] and a peak corresponding to the excited MC state appears in the UV−vis absorption spectra near 360 nm.

Deposition of the particles was studied using a Leica SP2 confocal and multiphoton microscope. Because of the weak fluorescence signal of the derivatized particles, confocal mi-

* Corresponding authors. E-mail: nsbell@sandia.gov (N.S.B.); pbraun@uiuc.edu (P.V.B.).

[†] Sandia National Laboratories.

[‡] University of Illinois at Urbana-Champaign.

(1) Huie, J. C. *Smart Mater. Struct.* **2003**, *12*, 264−271.
(2) Xia, Y.; Yin, Y.; Lu, Y.; McLellan, J. *Adv. Funct. Mater.* **2003**, *13*, 907−918.
(3) Xu, J.; O'Keefe, E. S.; Perry, C. C. *Mater. Lett.* **2004**, *58*, 3419−3423.
(4) Friebel, S.; Aizenberg, J.; Abad, S.; Wiltzius, P. *Appl. Phys. Lett.* **2000**, *77*, 2406−2408.
(5) Krueger, C.; Jonas, U. *J. Colloid Interface Sci.* **2002**, *252*, 331−338.
(6) Jonas, U.; Campo, A.; Krueger, C.; Glasser, G.; Boos, D. *Proc. Natl. Acad. Sci. U.S.A.* **2002**, *99*, 5034−5039.
(7) Aizenberg, J.; Braun, P. V.; Wiltzius, P. *Phys. Rev. Lett.* **2000**, *84*, 2997−3000.
(8) Mirkin, C. A. *Inorg. Chem.* **2000**, *39*, 2258−2272.
(9) Kim, S. H.; Misner, M. J.; Xu, T.; Kimura, M.; Russel, T. P. *Adv. Mater.* **2004**, *16*, 226−231.
(10) Brunner, M.; Bechinger, C. *Phys. Rev. Lett.* **2002**, *88*, 248302.
(11) Hoogenboom, J. P.; Vossen, D. L. J.; Faivre-Moskalenko, C.; Dogterom, M.; van Blaaderen, A. *Appl. Phys. Lett.* **2002**, *80*, 4828−4830.
(12) Hayward, R. C.; Saville, D. A.; Aksay, I. A. *Nature* **2000**, *404*, 56−59.
(13) Yellen, B. B.; Friedman, G. *Adv. Mater.* **2004**, *16*, 111−115.
(14) Van Blaaderen, A.; Ruel, R.; Wiltzius, P. *Nature* **1997**, *385*, 321−324.
(15) Lin, K. H.; Crocker, J. C.; Prasad, V.; Scohfield, A.; Weitz, D. A.; Lubensky, T. C.; Yodh, A. G. *Phys. Rev. Lett.* **2000**, *85*, 1770−1773.
(16) Braun, P. V.; Zehner, R. W.; White, C. A.; Weldon, M. K.; Kloc, C.; Patel, S. S.; Wiltzius, P. *Adv. Mater.* **2001**, *13*, 721−724.
(17) Yin, Y.; Xia, Y. *Adv. Mater.* **2002**, *14*, 605−608.
(18) Piech, M.; Bell, N. S. *Macromolecules*, in press.
(19) Matyjaszewski, K.; Miller, P. J.; Shukla, N.; Immaraporn, B.; Gelman, A.; Luokala, B. B.; Siclovan, T. M.; Kickelbick, G.; Vallant, T.; Hoffmann, H.; Pakula, T. *Macromolecules* **1999**, *32*, 8716−8724.
(20) Ma, Q.; Wooley, K. L. *J. Polym. Sci., Part A* **2000**, *38*, 4805−4820.
(21) Ejaz, M.; Tsujii, Y.; Fukuda, T. *Polymer* **2001**, *42*, 6811−6815.
(22) Masci, G.; Giacomelli, L.; Crescenzi, V. *Macromol. Rapid Commun.* **2004**, *25*, 559−564.
(23) Heiligman-Rim, R.; Hirshberg, Y.; Fisher, E. *J. Phys. Chem.* **1962**, *66*, 2465−2470.
(24) Bell, N. S.; Piech, M. *Langmuir*, in press.

10.1021/la051636c CCC: $33.50
Published on Web 01/11/2006

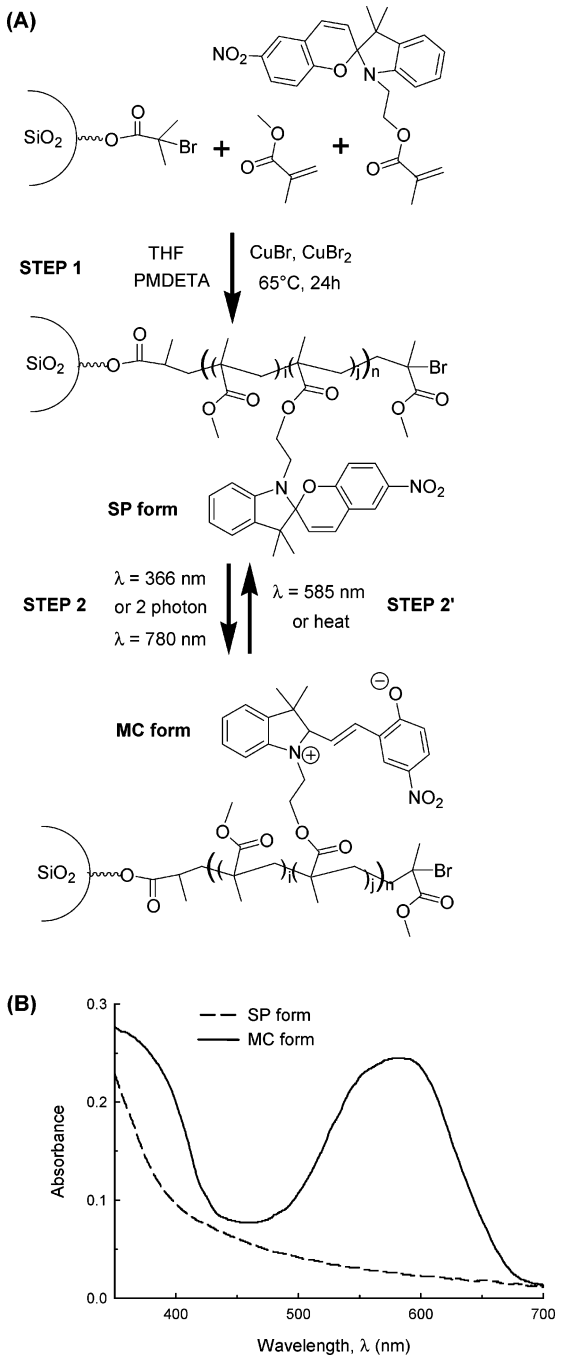

Figure 1. (A) Synthesis and photochemistry of the SP-*co*-MMA copolymer brush. Step 1: SP-*co*-MMA brush synthesis. Step 2: forward ring-opening reaction from closed SP to zwitterionic MC isomer facilitated by a single-photon UV or two-photon near-IR excitation. Step 2′: reverse reaction accelerated by heat or single-photon visible excitation. (B) UV−vis absorption spectra of 927 nm diameter SiO_2 colloids derivatized with an SP-*co*-MMA brush containing 20% SP and dispersed in toluene.

croscopy imaging was performed in reflectance mode. This microscope was also used to induce the SP-to-MC isomerization in the end-grafted SP-*co*-MMA copolymer brush films via a one-photon UV or multiphoton IR absorption process. By selectively blocking the beam, we photoswitched regions to the zwitterionic MC isomer for the selective adsorption of SP-*co*-MMA-coated, sterically stabilized colloids. Figure 2 shows an SP-*co*-MMA-modified quartz cover slip during the following experimental process. First, the surface was immersed in anhydrous toluene in a flow cell and imaged in reflectance mode using the 458 nm line of an argon ion laser. The polymer layer was then patterned using the mode-locked Ti−sapphire laser (λ = 780 nm, 100−150 fs pulse width, 82 MHz repetition rate) via a multiphoton absorption process.[25] The photoexcited SP molecules in the brush underwent the ring-opening reaction to give a MC isomer copolymer-covered surface.

Changes in the copolymer brush upon conversion from the SP to MC form enabled visualization of the lateral patterning via confocal reflectance imaging (λ = 458 nm) (Figure 2B). The MC isomer exhibits a low absorbance at this wavelength (Figure 1B), and thus the undesired reverse excitation of the MC isomer to the SP form was avoided.[26] The contrast in Figure 2B is likely due to changes in refractive index (i.e., $\Delta n > 0.0009$[27]) and thickness (i.e., up to 66% decrease in polymer thickness was observed upon UV irradiation for similar coatings in toluene[28]) in the irradiated film. However, further studies are required to definitively understand the observed reflectance contrast.

Following photopatterning, a well-dispersed 0.05 vol % (v/v) suspension of SP-*co*-MMA-copolymer-modified colloids in toluene was introduced into the flow cell at a rate of 0.37 mL/min via a syringe pump. The colloids settled toward the photopatterned quartz cover slip mounted at the cell bottom and preferentially adsorbed to the MC regions of the substrate (Figure 2C). It should be noted that colloidal suspension flow through the cell was relatively slow (∼1 cell vol min^{-1}), and the predominant particle transport toward the quartz surface occurred via sedimentation and diffusion. Following adsorption and rinsing with clean toluene, the flow cell was dried to determine whether the adsorption forces could withstand capillary drying stresses. As depicted in Figure 2D, the colloid patterning withstood these drying forces. However, during the drying process, particles remaining in the suspension were drawn toward the areas containing previously adsorbed colloids, which resulted in clustering. One might expect toluene to preferentially wet the nonpolar SP regions, which could induce disruptive forces at the edges of features during the drying. In our case, however, adsorbed particles were retained on the MC-switched regions, verifying strong colloid−surface adhesion.

Following adsorption experiments, particle density was compared in the MC and SP regions of the substrate using the fractional surface coverage parameter, $\theta = \pi a^2 N_p$. Here, N_p denotes the number of adsorbed colloids per unit area, and πa^2 represents the particle cross-sectional area. The analySIS image analysis package (Soft Imaging System GmbH) was used to count colloids in the captured images. Particles that did not change their position because of the solvent flow, Brownian motion, or surface diffusion were considered adhered to the surface. The results of this analysis for two experiments differing only in the concentration of colloidal suspension employed are reported in Table 1.

It is informative to compare the initial adsorption rate onto the MC regions (θ'_{MC}) with the flux of sedimenting particles toward the surface (θ'_{th}) determined using Stokes' law. At both volume fractions, these quantities were very similar, implying an irreversible adsorption process. Conversely, the initial adsorption rate onto the SP regions was found to be 9−14 times lower than the adsorption rate on MC regions, indicating high particle mobility. Furthermore, this difference in initial adsorption behavior onto MC and SP regions was not affected by the particle concentration in the cell (i.e., 0.01−0.1% v/v) and employed

(25) Parthenopoulos, S. A.; Rentzepis, P. M. *Science* **1989**, *245*, 843−845.
(26) Tork, A.; Boudreault, F.; Roberge, M.; Ritcey, A. M.; Lessard, R. A.; Galstian, T. V. *Appl. Opt.* **2001**, *40*, 1180−1186.
(27) Kim, E.; Choi, Y. K.; Lee, M. H.; Han, S. G.; Keum, S. R. *J. Korean Phys. Soc.* **1999**, *35*, S615−S617.
(28) Park, Y. S.; Ito, Y.; Imanishi, Y. *Macromolecules* **1998**, *31*, 2606−2610.

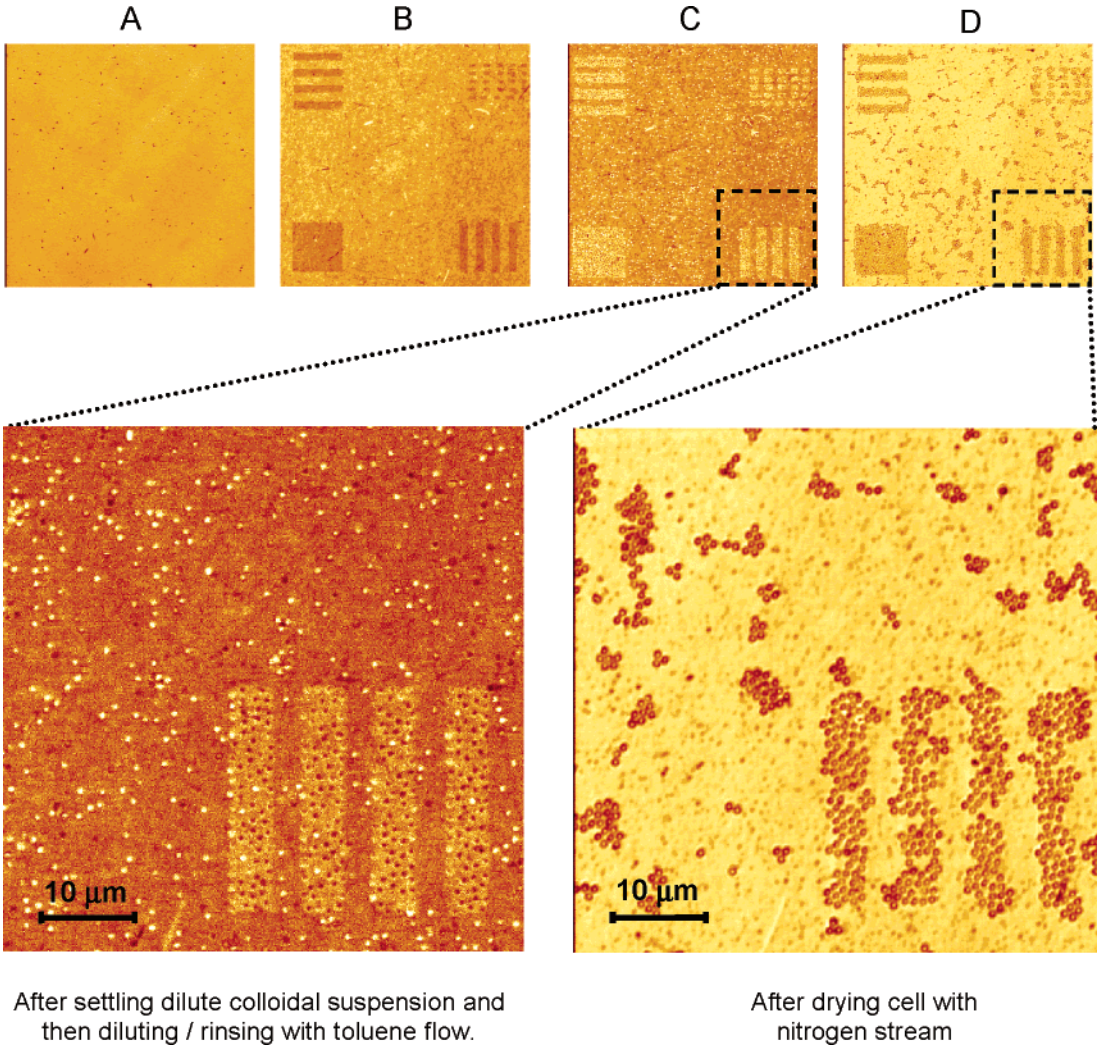

Figure 2. Reflectance confocal microscope images of an adsorption experiment. The SP-*co*-MMA-copolymer-coated quartz cover slip was (A) immersed in toluene and (B) exposed to the focused 780 nm pulsed laser beam to pattern substrate regions with the MC isomer via a two-photon process. (C) Following the introduction of SP-*co*-MMA-copolymer-derivatized colloids into the cell and rinsing with clean toluene, colloids were preferentially adsorbed onto the MC-patterned regions. (D) Image after drying using a nitrogen stream.

Table 1. Image Analysis Summary for Two Adsorption Experiments Carried out in the Flow Cell with a Flow Rate of 0.37 mL/min[a]

		photoswitched regions			unexposed regions			
expt	concn % v/v	θ'_{MC}[b] ($\times 10^4$ s^{-1})	$\theta_{MC,ads}$[c]	$\theta_{MC,dry}$[d]	θ'_{SP} ($\times 10^4$ s^{-1})	$\theta_{SP,ads}$	$\theta_{SP,dry}$	θ'_{th}[e] ($\times 10^4$ s^{-1})
A	0.05	8.8 ± 0.3	0.492	0.538	0.64 ± 0.02	0.123	0.053	7.8
B	0.01	1.5 ± 0.1	0.478	0.514	0.16 ± 0.01	0.04	0.04	1.6

[a] The adsorption process onto photoswitched and unexposed regions was followed with a confocal microscope. [b] θ' denotes the initial adsorption rate, $d\theta/dt$, obtained from the slope of θ vs time graph, which is linear for $\theta < 0.2$ (see Figure 3). The subscripts MC and SP represent photoexposed and unexposed regions of the surface, respectively. [c] Fractional surface coverage following the adsorption and rinsing steps. [d] Fractional surface coverage after surface drying. [e] Theoretical flux of particles toward the substrate defined as $\theta'_{th} = \rho_b \times \upsilon_{sed} \times \pi a^2$. Here, ρ_b denotes the particle number concentration in the bulk, and υ_{sed} stands for the particle settling velocity calculated using the Stokes' law and based on the polymer-coated particle diameter, a.

flow rates (i.e., 0−1 mL/min). During later stages of the adsorption process, however, more concentrated suspensions and slower flow rates tended to decrease adsorption selectivity toward the MC regions. Thus, after colloidal adsorption and cell rinsing, selectivity (defined by the ratio $\theta_{MC,ads}/\theta_{SP,ads}$) was only 4.0 with 0.05% v/v suspension flown through the cell (expt A in Table 1). Decreasing the particle concentration to 0.01% v/v gave $\theta_{MC,ads}/\theta_{SP,ads} = 12.1$ (expt B in Table 1). It should also be noted that surface coverage in MC regions approached the value of 1/2. This is below the random sequential adsorption jamming limit ($\theta_{RSA} \approx 0.547 \pm 0.002$) predicted by Monte Carlo simulations[29] and further corroborates the irreversible nature of the adsorption process examined here. Furthermore, data presented in Table 1 indicate densification of the colloidal deposit upon drying (i.e., $\theta_{MC,dry} > \theta_{MC,ads}$) due to capillary stresses.

Adsorption kinetics for experiment A are illustrated in Figure 3. During the initial stage corresponding to unobstructed particle deposition, the plots are linear, yielding a constant adsorption rate for $\theta < 0.2$. This initial adsorption rate onto the MC regions (θ'_{MC}) is very similar to the flux of sedimenting particles toward

(29) Evans, J. W. *Rev. Mod. Phys.* **1993**, *65*, 1281−1329.

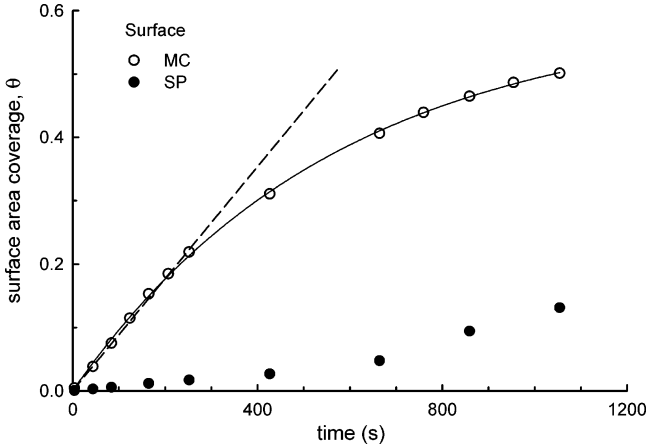

Figure 3. Plot of fractional surface coverage as a function of time for colloids depositing onto the photoswitched (MC) and unexposed (SP) regions of the substrate modified with an SP-*co*-MMA copolymer brush. Experimental details are summarized in the caption of Figure 2 and Table 1 (expt A). The solid line represents the mean-field model fit (eq 1), while the broken line describes the flux of sedimenting particles toward the surface determined from Stokes' law.

the surface (θ'_{th}) determined using Stokes' law (see Table 1) and points to irreversible adsorption. In the SP regions, on the other hand, the adsorption rate was significantly lower because of colloids diffusing along the surface before being captured.

Because of the coupling between sedimentation and diffusion, along with particle accumulation next to the surface, random sequential adsorption[30] and ballistic deposition[31] models cannot be used to quantitatively describe the experimental data. The adsorption process in the photoswitched regions (MC) was instead compared to the mean-field theory of irreversible multilayer adsorption[32] up to the monolayer coverage. The kinetic law describing the evolution of the adsorption process in the first layer is of the form

$$\theta(t) = \Lambda(1 - e^{-St/\Lambda}) \qquad (1)$$

where Λ denotes the maximum surface coverage in the first layer, and S denotes the deposition rate. The data in Figure 3 was fit to this model using Λ and S as free parameters, giving $\Lambda = 0.597 \pm 0.007$, $S = (1.05 \pm 0.02) \times 10^{-3}\ s^{-1}$, with $R^2 = 0.9999$. The value of Λ falls between that expected of random sequential adsorption (i.e., $\Lambda_{RSA} = 0.547$[29]) and ballistic deposition (i.e., $\Lambda_{BD} = 0.610$[33]), while S is similar in magnitude to the particle sedimentation rate (i.e., $8.8 \times 10^{-3}\ s^{-1}$). It should be mentioned that, because of the reversible nature of the absorption process in the SP regions of the surface (i.e., particles were observed to adsorb, desorb, and diffuse freely along the substrate), fitting of the kinetic data to the mean-field model was not attempted.

The significant difference in the adsorption behavior between the MC and SP regions of the surface points to strong attractive interactions between the colloids and the photoirradiated surface. The nature of this attraction is still open to debate. In the past, strong UV-induced aggregation had been reported for silica particles modified with covalently tethered alkyl chains possessing terminal SP groups.[34,35] The authors ascribed the enhanced flocculation and sedimentation of the photoswitched colloids to the increase in surface polarity. Specifically, abrupt reduction in interaction between polar MCs and nonpolar solvent molecules resulted in strong attraction between MC moieties on neighboring particles bringing about the reported aggregation. In a related investigation, a decrease in polymer−solvent interaction has been used to explain the UV-induced precipitation of polystyrene with SP pendant groups in cyclohexane.[36] In another example, conformational changes of SP-derivatized poly(methyl methacrylate) in benzene were attributed to specific intramolecular interactions between ester groups of the polymer and UV-generated MCs.[37] Finally, the formation of MC_n intrachain molecular aggregates in different polymers containing SP side groups has been linked to macromolecular coil shrinking and interesting crystallization behavior.[38] In our observations, the strong affinity between the polymer brush-coated colloids and surfaces when only one of them is photoswitched cannot be attributed to MC−MC interactions or electrostatic forces (only one of the surfaces is polar and zwitterionic, while the other remains neutral.) Moreover, thick polymer layers provide steric stabilization and minimize van der Waals attraction. One possibility is that SP−MC aggregation within intercalated polymer brushes holds the surfaces together. Further studies of this photoswitchable system are necessary to gain better understanding of the interaction mechanism.

In summary, we have demonstrated a system for photodefining regions of increased polarity in SP-*co*-MMA films onto which SP-*co*-MMA-modified colloids adsorb preferentially. Deposition kinetics and coverage saturation below the random sequential deposition jamming limit indicate irreversible adsorption onto the photoswitched substrate regions. This technique demonstrates the potential for direct pattern formation without the need for photolithography. In the future, we plan to test the limits of this technique by creating patterns on the order of the single-particle diameter. Moreover, we hope to explore reversible sticking of colloids by promoting the opposite isomerization reaction (MC to SP) by visible wavelengths. The reversible polarity change could allow more precise particle adsorption and thus provide a route to novel material fabrication with precise defect placement.

Acknowledgment. Funding was supplied for this work through the Sandia National Laboratories LDRD program, the Center for Integrated Nanotechnologies, the U.S. DOE, Division of Materials Sciences under Award No. DEFG02-91ER45439, and through the Frederick Seitz Materials Research Laboratory at the University of Illinois at Urbana-Champaign. Sandia National Laboratories is a multiprogram laboratory operated by Sandia Corporation, a Lockheed Martin Company. This work was supported by the U.S. DOE under contract DE-AC04-94AL85000.

Supporting Information Available: Description of synthesis procedures. This material is available free of charge via the Internet at http://pubs.acs.org.

LA051636C

(30) Schaaf, P.; Talbot, J. *Phys. Rev. Lett.* **1989**, *62*, 175−178.
(31) Choi, H. S.; Talbot, J.; Tarjus, G.; Viot, P. *J. Chem. Phys.* **1993**, *99*, 9296−9303.
(32) Privman, V.; Frisch, H. L.; Ryde, N.; Matijević, E. *J. Chem. Soc., Faraday Trans.* **1991**, *87*, 1371−1375.
(33) Jullien, R.; Meakin, P. *J. Phys. A: Math. Gen* **1992**, *25*, L189−L194.
(34) Ueda, M.; Kim, H. B.; Ichimura, K. *J. Mater. Chem.* **1994**, *4*, 883−889.
(35) Ueda, M.; Kudo, K.; Ichimura, K. *J. Mater. Chem.* **1995**, *5*, 1007−1011.
(36) Irie, M.; Iwayanagi, T.; Taniguchi, Y. *Macromolecules* **1985**, *18*, 2418−2422.
(37) Irie, M.; Menju, A.; Hayashi, K. *Macromolecules* **1979**, *12*, 1176−1180.
(38) Goldburt, E.; Shvartsman, F.; Fishman, S.; Krongauz, V. *Macromolecules* **1984**, *17*, 1225−1230.